Available online at www.sciencedirect.com
SCIENCE DIRECT®
Journal of Sound and Vibration 282 (2005) 277–296
JOURNAL OF SOUND AND VIBRATION
www.elsevier.com/locate/jsvi

Three-dimensional vibration analysis of thick hyperboloidal shells of revolution

Jae-Hoon Kang[a,*], Arthur W. Leissa[b]

[a]*Department of Architectural Engineering, College of Engineering, Chung-Ang University, Seoul, Korea*
[b]*Department of Mechanical Engineering, Colorado State University, Fort Collins, CO, USA*

Received 26 June 2003; accepted 19 February 2004
Available online 17 September 2004

Abstract

A three-dimensional (3-D) method of analysis is presented for determining the free vibration frequencies and mode shapes of thick, hyperboloidal shells of revolution. Unlike conventional shell theories, which are mathematically two-dimensional (2-D), the present method is based upon the 3-D dynamic equations of elasticity. Displacement components u_r, u_θ, and u_z in the radial, circumferential, and axial directions, respectively, are taken to be sinusoidal in time, periodic in θ, and algebraic polynomials in the r and z directions. Potential (strain) and kinetic energies of the hyperboloidal shells are formulated, and the Ritz method is used to solve the eigenvalue problem, thus yielding upper bound values of the frequencies by minimizing the frequencies. As the degree of the polynomials is increased, frequencies converge to the exact values. Convergence to four-digit exactitude is demonstrated for the first five frequencies of the hyperboloidal shells of revolution. Numerical results are tabulated for 18 configurations of completely free hyperboloidal shells of revolution having two different shell thickness ratios, three variant axis ratios, and three types of shell height ratios. Poisson's ratio (ν) is fixed at 0.3. Comparisons are made among the frequencies for these hyperboloidal shells and ones which are cylindrical or nearly cylindrical (small meridional curvature). The method is applicable to thin hyperboloidal shells, as well as thick and very thick ones.

*Corresponding author. Tel.: +82-2-820-5342; fax: +82-2-812-4150.
E-mail address: jhkang@cau.ac.kr (J.-H. Kang).

0022-460X/$ - see front matter © 2004 Elsevier Ltd. All rights reserved.
doi:10.1016/j.jsv.2004.02.031

1. Introduction

Hyperboloidal shell types of structures have been used widespread both in industrial and public buildings; for example, cooling towers, water towers, TV towers, supports of electric power transmission lines, reinforced concrete water vessels, high factory chimneys, and so forth, since they give rise to optimum conditions for good aerodynamics, strength, and stability.

A vast published literature exists for free vibrations of shells. The monograph of Leissa [1] summarized approximately 1000 relevant publications world-wide through the 1960s. Almost all of these dealt with shells of revolution (e.g., circular cylindrical, conical, spherical). Among them were three references [2–4] considering hyperboloidal shells of revolution (see p. 412 in Ref. [1]). A recent review article by Krivoshapko [5] describes some additional research on free vibrations of hyperboloidal shells of revolution for the period 1975–2000.

However, these analyses [2–4, 6–22] were based upon shell theory, which is mathematically two-dimensional (2-D). That is, for thin shells one assumes the Kirchhoff hypothesis that normals to the shell middle surface remain normal to it during deformations (vibratory, in this case), and unstretched in length. This yields an eighth-order set of partial differential equations of motion. For hyperboloidal shells they involve variable coefficients, making them quite difficult to solve.

Even so, conventional shell theory is only applicable to thin shells. A higher order shell theory could be derived, which considers the effects of shear deformation and rotary inertia, and would be useful for the low-frequency modes of moderately thick shells. Such a theory would also be 2-D. But for hyperboloidal shells the resulting equations would be very complicated.

Three-dimensional (3-D) analysis of structural elements has long been a goal of those who work in the field. With the current availability of computers of increased speed and capacity, it is now possible to perform 3-D structural analyses of bodies to obtain accurate values of static displacements, free vibration frequencies and mode shapes, and buckling loads and mode shapes.

In the present work, hyperboloidal shells of revolution are analyzed by a 3-D approach. Instead of attempting to solve equations of motion, an energy approach is followed which, as sufficient freedom is given to the three displacement components, yields frequency values as close to the exact ones as desired. To evaluate the energy integrations over the shell volume exactly (not numerically), displacements and strains are expressed in terms of the circular cylindrical coordinates, instead of related 3-D shell coordinates which are normal and tangential to the shell midsurface. Results are obtained for hyperboloidal shells of revolution with constant thickness along the radial direction (r) and completely free. These data serve as benchmarks against which other approximate methods (e.g., finite elements, finite differences) and other improved 2-D shell theories may be tested.

2. Method of analysis

A representative cross section of hyperboloidal shells of revolution of constant thickness (h) in the radial direction (r), and height H ($= H_t + H_b$) of the shell in the axial direction (z), where H_t and H_b are the lengths from the r-axis to the top and bottom ends of the shell, respectively, is shown in Fig. 1. If the shell thickness is defined as normal thickness to the midsurface of the shell, this shell has a thickness variation in the meridional direction. The lengths of major and minor

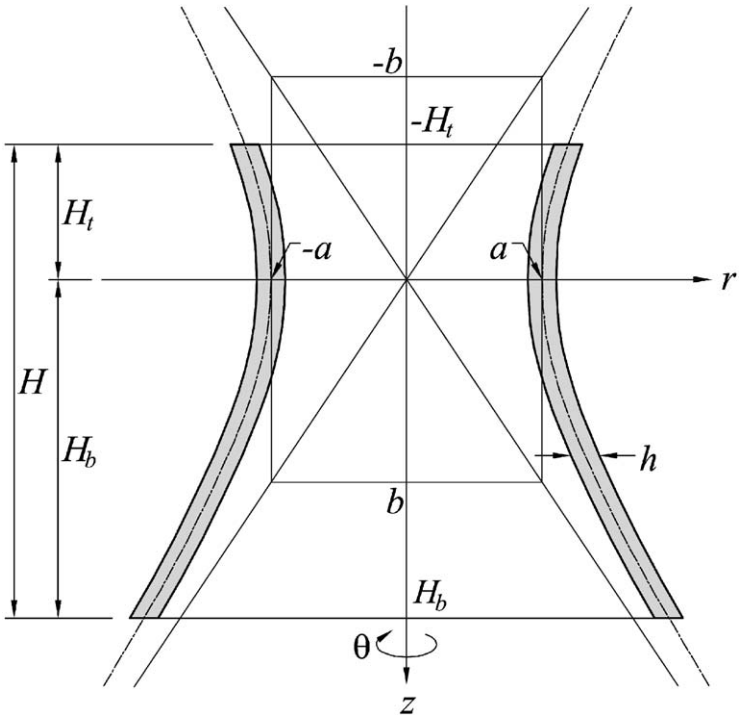

Fig. 1. A representative hyperboloidal shell of revolution with the cylindrical coordinate system (r, θ, z).

axes of the mid-surface of the hyperboloidal shell are $2a$ and $2b$, respectively, and so slopes of asymptotes are $\pm b/a$. The cylindrical coordinate system (r, θ, z), also shown in the figure, is used in the analysis, where θ is the circumferential angle. The equation of the hyperboloidal mid-surface is $(r/a)^2 - (z/b)^2 = 1$. Thus, the domain of the shell is given by

$$\frac{a}{b}\sqrt{z^2+b^2} - \frac{h}{2} \leqslant r \leqslant \frac{a}{b}\sqrt{z^2+b^2} + \frac{h}{2}, \quad 0 \leqslant \theta \leqslant 2\pi, \quad -H_t \leqslant z \leqslant H_b. \tag{1}$$

Utilizing tensor analysis (cf. Ref. [23]), the three equations of motion in the cylindrical coordinate system (r, θ, z) are found to be

$$\sigma_{rr,r} + \sigma_{rz,z} + \frac{1}{r}(\sigma_{rr} - \sigma_{\theta\theta} + \sigma_{r\theta,\theta}) = \rho\ddot{u}_r, \tag{2a}$$

$$\sigma_{r\theta,r} + \sigma_{\theta z,z} + \frac{1}{r}(2\sigma_{r\theta} + \sigma_{\theta\theta,\theta}) = \rho\ddot{u}_\theta, \tag{2b}$$

$$\sigma_{rz,r} + \sigma_{zz,z} + \frac{1}{r}(\sigma_{rz} + \sigma_{\theta z,\theta}) = \rho\ddot{u}_z, \tag{2c}$$

where the σ_{ij} are the normal ($i = j$) and shear ($i \neq j$) stress components; u_r, u_θ, and u_z are the displacement components in the r, θ, and z directions, respectively; ρ is mass density per unit volume; the commas indicate spatial derivatives; and the dots denote time derivatives.

The well-known relationships between the tensorial stresses (σ_{ij}) and strains (ε_{ij}) of isotropic, linear elasticity are

$$\sigma_{ij} = \lambda\varepsilon\delta_{ij} + 2G\varepsilon_{ij}, \tag{3}$$

where λ and G are the Lamé parameters, expressed in terms of Young's modulus (E) and Poisson's ratio (v) for an isotropic solid as

$$\lambda = \frac{Ev}{(1+v)(1-2v)}, \quad G = \frac{E}{2(1+v)}, \tag{4}$$

$\varepsilon \equiv \varepsilon_{rr} + \varepsilon_{\theta\theta} + \varepsilon_{zz}$ is the trace of the strain tensor, and δ_{ij} is Kronecker's delta.

The 3-D tensorial strains (ε_{ij}) are found to be related to the three displacements u_r, u_θ, and u_z, by (cf. Ref. [23])

$$\varepsilon_{rr} = u_{r,r}, \quad \varepsilon_{\theta\theta} = \frac{u_{\theta,\theta} + u_r}{r}, \quad \varepsilon_{zz} = u_{z,z}, \tag{5a–c}$$

$$\varepsilon_{r\theta} = \frac{1}{2}\left[u_{\theta,r} + \frac{u_{r,\theta} - u_\theta}{r}\right], \quad \varepsilon_{rz} = \tfrac{1}{2}(u_{r,z} + u_{z,r}), \quad \varepsilon_{\theta z} = \frac{1}{2}\left[u_{\theta,z} + \frac{u_{z,\theta}}{r}\right]. \tag{5d–f}$$

Substituting Eqs. (3) and (5) into Eq. (2), one obtains a set of second-order partial differential equation in u_r, u_θ, and u_z governing free vibrations. However, in the case of hyperboloidal shells, exact solutions are intractable because of the variable coefficients that appear in many terms. Alternatively, one may approach the problem from an energy perspective.

During vibratory deformation of the body, its strain (potential) energy (V) is the integral over the domain (Ω):

$$V = \tfrac{1}{2}\int_\Omega (\sigma_{rr}\varepsilon_{rr} + \sigma_{\theta\theta}\varepsilon_{\theta\theta} + \sigma_{zz}\varepsilon_{zz} + 2\sigma_{r\theta}\varepsilon_{r\theta} + 2\sigma_{rz}\varepsilon_{rz} + 2\sigma_{\theta z}\varepsilon_{\theta z})r\,\mathrm{d}r\,\mathrm{d}\theta\,\mathrm{d}z. \tag{6}$$

Substituting Eqs. (3) and (5) into Eq. (6) results in the strain energy in terms of the three displacements:

$$V = \tfrac{1}{2}\int_\Omega [\lambda(\varepsilon_{rr} + \varepsilon_{\theta\theta} + \varepsilon_{zz})^2 + 2G\{\varepsilon_{rr}^2 + \varepsilon_{\theta\theta}^2 + \varepsilon_{zz}^2 + 2(\varepsilon_{r\theta}^2 + \varepsilon_{rz}^2 + \varepsilon_{\theta z}^2)\}]r\,\mathrm{d}r\,\mathrm{d}\theta\,\mathrm{d}z, \tag{7}$$

where the tensorial strains ε_{ij} are expressed in terms of the three displacements by Eq. (5).

The kinetic energy (T) is simply

$$T = \tfrac{1}{2}\int_\Omega \rho(\dot{u}_r^2 + \dot{u}_\theta^2 + \dot{u}_z^2)r\,\mathrm{d}r\,\mathrm{d}\theta\,\mathrm{d}z. \tag{8}$$

For mathematical convenience, the radial r and axial z coordinates are made dimensionless as $\psi \equiv r/h$ and $\zeta \equiv z/H$. Thus, the ranges of the nondimensional cylindrical coordinates (ψ, θ, ζ) are given by

$$\psi_1(\zeta) \leqslant \psi \leqslant \psi_2(\zeta), \quad 0 \leqslant \theta \leqslant 2\pi, \quad -\frac{H_t}{H} \leqslant \zeta \leqslant \frac{H_b}{H}, \tag{9}$$

where

$$\psi_1(\zeta) \equiv \frac{\sqrt{(H^*\zeta)^2 + k^2}}{kh^*} - \frac{1}{2}, \tag{10a}$$

$$\psi_2(\zeta) \equiv \frac{\sqrt{(H^*\zeta)^2 + k^2}}{kh^*} + \frac{1}{2} \tag{10b}$$

and $H^*(\equiv H/a)$ and $h^*(\equiv h/a)$ are the nondimensional height and thickness of the shell, respectively, and $k(\equiv b/a)$ is the axis ratio (and asymptote slope).

For the free, undamped vibration, the time (t) response of the three displacements is sinusoidal and, moreover, the circular symmetry of the body allows the displacements to be expressed by

$$u_r(\psi, \theta, \zeta, t) = U_r(\psi, \zeta)\cos n\theta \, \sin(\omega t + \alpha), \tag{11a}$$

$$u_\theta(\psi, \theta, \zeta, t) = U_\theta(\psi, \zeta)\sin n\theta \, \sin(\omega t + \alpha) \tag{11b}$$

$$u_z(\psi, \theta, \zeta, t) = U_z(\psi, \zeta)\cos n\theta \, \sin(\omega t + \alpha), \tag{11c}$$

where U_r, U_θ, and U_z are displacement functions of ψ and ζ, ω is a natural frequency, and α is an arbitrary phase angle determined by the initial conditions. The circumferential wave number is taken to be an integer ($n = 0, 1, 2, 3, \ldots, \infty$), to ensure periodicity in θ. Then Eq. (11) accounts for all free vibration modes except for the torsional ones. These modes arise from an alternative set of solutions which are the same as in Eq. (11), except that $\cos n\theta$ and $\sin n\theta$ are interchanged. For $n > 0$, this set duplicates the solutions of Eq. (11), with the symmetry axes of the mode shapes being rotated. But for $n = 0$ the alternative set reduces to $u_r = u_z = 0$, $u_\theta = U_\theta^*(r, z)\sin(\omega t + \alpha)$, which corresponds to the torsional modes. The displacements uncouple by circumferential wavenumber (n), leaving only coupling in r and z.

The Ritz method uses the maximum potential (strain) energy ($V_{\max}$) and the maximum kinetic energy ($T_{\max}$) functionals in a cycle of vibratory motion. The functionals are obtained by setting $\sin^2(\omega t + \alpha)$ and $\cos^2(\omega t + \alpha)$ equal to unity in Eqs. (7) and (8) after the displacements (11) are substituted, and by using the nondimensional coordinates ψ and ζ as follows:

$$V_{\max} = \frac{GH}{2}\int_{-H_t/H}^{H_b/H}\int_{\psi_1}^{\psi_2}\left[\left\{\frac{\lambda}{G}(\kappa_1 + \kappa_2 + \kappa_3)^2 + 2(\kappa_1^2 + \kappa_2^2 + \kappa_3^2) + \kappa_4^2\right\}\Gamma_1 + (\kappa_5^2 + \kappa_6^2)\Gamma_2\right]\psi \, \mathrm{d}\psi \, \mathrm{d}\zeta, \tag{12}$$

$$T_{\max} = \frac{\rho H h^2 \omega^2}{2}\int_{-H_t/H}^{H_b/H}\int_{\psi_1}^{\psi_2}[(U_r^2 + U_z^2)\Gamma_1 + U_\theta^2\Gamma_2]\psi \, \mathrm{d}\psi \, \mathrm{d}\zeta, \tag{13}$$

where

$$\kappa_1 \equiv \frac{U_r + nU_\theta}{\psi}, \quad \kappa_2 \equiv \frac{h^*}{H^*}U_{z,\zeta}, \quad \kappa_3 \equiv U_{r,\psi}, \tag{14a}$$

$$\kappa_4 \equiv \frac{h^*}{H^*}U_{r,\zeta} + U_{z,\psi}, \quad \kappa_5 \equiv \frac{U_\theta + nU_r}{\psi} - U_{\theta,\psi}, \quad \kappa_6 \equiv \frac{nU_z}{\psi} - \frac{h^*}{H^*}U_{\theta,\zeta} \tag{14b}$$

and Γ_1 and Γ_2 are constants, defined by

$$\Gamma_1 \equiv \int_0^{2\pi} \cos^2 n\theta \mathrm{d}\theta = \begin{cases} 2\pi & \text{if } n = 0, \\ \pi & \text{if } n \geqslant 1, \end{cases} \quad \Gamma_2 \equiv \int_0^{2\pi} \sin^2 n\theta \mathrm{d}\theta = \begin{cases} 0 & \text{if } n = 0, \\ \pi & \text{if } n \geqslant 1. \end{cases} \tag{15}$$

From Eq. (4), it is seen that the nondimensional constant λ/G in Eq. (12) involves only v; i.e.,

$$\frac{\lambda}{G} = \frac{2v}{1-2v}. \tag{16}$$

The displacement functions U_r, U_θ, and U_z in Eq. (11) are further assumed as algebraic polynomials,

$$U_r(\psi,\zeta) = \eta_r(\psi,\zeta) \sum_{k=0}^{K} \sum_{l=0}^{L} A_{ij} \psi^i \zeta^j, \tag{17a}$$

$$U_\theta(\psi,\zeta) = \eta_\theta(\psi,\zeta) \sum_{k=0}^{K} \sum_{l=0}^{L} B_{kl} \psi^k \zeta^l, \tag{17b}$$

$$U_z(\psi,\zeta) = \eta_z(\psi,\zeta) \sum_{m=0}^{M} \sum_{n=0}^{N} C_{mn} \psi^m \zeta^n \tag{17c}$$

and similarly for U_θ^*, where i, j, k, l, m, and n are integers; I, J, K, L, M, and N are the highest degrees taken in the polynomial terms; A_{ij}, B_{kl} and C_{mn} are arbitrary coefficients to be determined, and the η are functions depending upon the geometric boundary conditions to be enforced. For example: (1) completely free: $\eta_r = \eta_\theta = \eta_z = 1$; (2) bottom end ($z = H_b$) fixed, remaining boundaries free: $\eta_r = \eta_\theta = \eta_z = \zeta - H_b/H$; (3) top end ($z = -H_t$) fixed, remaining boundaries free: $\eta_r = \eta_\theta = \eta_z = \zeta + H_t/H$; (4) both ends fixed: $\eta_r = \eta_\theta = \eta_z = (\zeta - H_b/H)(\zeta + H_t/H)$.

The functions of η shown above impose only the necessary geometric constraints. Together with the algebraic polynomials in Eq. (17), they form function sets which are mathematically complete (cf., Ref. [24] pp. 266–268). Thus, the function sets are capable of representing any 3-D motion of the body with increasing accuracy as the indices $I, J, \ldots, N$ are increased. In the limit, as sufficient terms are taken, all internal kinematic constraints vanish, and the functions (17) will approach the exact solution as closely as desired.

The eigenvalue problem is formulated by minimizing the free vibration frequencies with respect to the arbitrary coefficients A_{ij}, B_{kl} and C_{mn}, thereby minimizing the effects of the internal constraints present, when the function sets are finite. This corresponds to the following equations [25]:

$$\frac{\partial}{\partial A_{ij}}(V_{\max} - T_{\max}) = 0, \quad i = 0,1,2,...,I;\ j = 0,1,2,...,J, \tag{18a}$$

$$\frac{\partial}{\partial B_{kl}}(V_{\max} - T_{\max}) = 0, \quad k = 0,1,2,...,K;\ l = 0,1,2,...,L, \tag{18b}$$

$$\frac{\partial}{\partial C_{mn}}(V_{\max} - T_{\max}) = 0, \quad m = 0,1,2,...,M;\ n = 0,1,2,...,N. \tag{18c}$$

Eq. (18) yields a set of $(I+1)(J+1)+(K+1)(L+1)+(M+1)(N+1)$ linear, homogeneous, algebraic equations in the unknowns A_{ij}, B_{kl} and C_{mn}. For a nontrivial solution, the determinant of the coefficient matrix is set equal to zero, which yields the frequencies (eigenvalues). These frequencies are upper bounds on the exact values. The mode shape (eigenfunction) corresponding to each frequency is obtained, in the usual manner, by substituting each ω back into the set of algebraic equations, and solving for the ratios of coefficients.

3. Convergence studies

To establish the accuracy of frequencies obtained by the procedure described above, it is necessary to conduct some convergence studies to determine the number of terms required in the power series of Eq. (17). A convergence study is based upon the fact that all the frequencies obtained by the Ritz method should converge to their exact values in an upper bound manner when the mathematically complete set of polynomials in Eq. (17) are used. If the results were not to converge properly, or to converge too slowly, it is likely that the assumed displacements may be poor choices, or be missing some functions from a minimal complete set of polynomials.

Table 1 is such a study for a completely free, hyperboloidal shell of revolution with $b/a=1$, $H_b/a=4$, $H_t/H_b=0$, and $h/a=0.2$, depicted as the first configuration in Fig. 2. The table lists the first five nondimensional frequencies in $\omega a\sqrt{\rho/G}$ with $\nu=0.3$ for bending modes ($n=2$).

To make the study of convergence less complicated, equal numbers of polynomial terms were taken in both the r (or ψ) coordinate (i.e., $I=K=M$) and z (or ζ) coordinate (i.e., $J=L=N$), although some computational optimization could be obtained for some configurations and some mode shapes by using an unequal number of polynomial terms.

The symbols TR and TZ in the table indicate the total numbers of polynomial terms used in the r (or ψ) and z (or ζ) directions, respectively. Note that the frequency determinant order DET is related to TR and TZ as follows:

$$\mathrm{DET}=\begin{cases}\mathrm{TR}\times\mathrm{TZ} & \text{for torsional modes } (n=0),\\ 2\times\mathrm{TR}\times\mathrm{TZ} & \text{for axisymmetric modes } (n=0),\\ 3\times\mathrm{TR}\times\mathrm{TZ} & \text{for general modes } (n\geqslant 1).\end{cases}\tag{19}$$

Table 1 shows the monotonic convergence of all five frequencies as TR ($=I+1$, $K+1$ and $M+1$ in Eq. (17)) is increased, as well as TZ ($=J+1$, $L+1$ and $N+1$ in Eq. (17)). One sees, for example, that the fundamental (i.e., lowest) nondimensional frequency $\omega a\sqrt{\rho/G}$ converges to four digits (0.02871) when as few as $(5\times 12)=60$ terms are used, which results in DET = 180. Moreover, this accuracy requires using at least five terms through the radial (TR = 5) and twelve through the axial direction (TZ = 12). Numbers in underlined, bold-face type in Table 1 are the most accurate values (i.e., least upper bounds) achieved with the smallest determinant sizes.

Table 2 is a similar convergence study for the bending modes for $n=2$ of a thicker, hyperboloidal shell of revolution having less meridional curvature, with $b/a=3$, $H_t/H_b=1$,

Table 1
Convergence of frequencies in $\omega a\sqrt{\rho/G}$ of a completely free hyperboloidal shell of revolution for the five lowest bending modes ($n=2$) with $b/a=1$, $h/a=0.2$, $H_b/a=4$, and $H_t/H_b=0$ ($\nu=0.3$)

TR	TZ	DET	1	2	3	4	5
2	2	12	0.06729	0.5756	0.8806	1.127	1.377
2	4	24	0.03690	0.1621	0.4344	0.6912	0.9963
2	6	36	0.03244	0.1452	0.3854	0.6346	0.7071
2	8	48	0.03190	0.1430	0.3799	0.5744	0.6903
2	10	60	0.03177	0.1428	0.3797	0.5675	0.6885
2	12	72	0.03173	0.1428	0.3796	0.5672	0.6885
3	2	18	0.05364	0.1980	0.6597	0.7940	1.040
3	4	36	0.03158	0.1286	0.3558	0.5691	0.6934
3	6	54	0.02932	0.1219	0.3323	0.4840	0.6787
3	8	72	0.02892	0.1206	0.3310	0.4556	0.6236
3	10	90	0.02880	0.1202	0.3307	0.4513	0.6059
3	12	108	0.02877	0.1202	0.3306	0.4511	0.6023
4	2	24	0.04458	0.1809	0.4750	0.6979	1.009
4	4	48	0.03025	0.1239	0.3360	0.5263	0.6886
4	6	72	0.02904	0.1209	0.3312	0.4568	0.6386
4	8	96	0.02881	0.1202	0.3306	0.4513	0.6076
4	10	120	0.02874	0.1201	0.3305	0.4506	0.6012
4	12	144	0.02872	0.1200	0.3304	0.4506	0.6006
5	2	30	0.04164	0.1623	0.4535	0.6951	0.8591
5	4	60	0.02962	0.1226	0.3320	0.4752	0.6753
5	6	90	0.02890	0.1205	0.3308	0.4523	0.6182
5	8	120	0.02876	0.1201	0.3305	0.4508	0.6018
5	10	150	0.02874	0.1201	0.3305	0.4506	0.6012
5	12	180	**0.02871**	0.1200	0.3304	**0.4505**	0.6005
5	13	195	0.02871	0.1200	**0.3303**	0.4505	**0.6003**
6	2	36	0.04016	0.1572	0.4183	0.6649	0.7255
6	4	72	0.02920	0.1215	0.3313	0.4590	0.6484
6	6	108	0.02882	0.1203	0.3306	0.4510	0.6051
6	8	144	0.02874	0.1201	0.3305	0.4506	0.6010
6	10	180	0.02872	0.1200	0.3304	0.4506	0.6006
6	12	216	0.02871	0.1200	0.3303	0.4505	0.6005
7	2	42	0.03877	0.1560	0.4117	0.6497	0.7075
7	4	84	0.02904	0.1209	0.3309	0.4534	0.6245
7	6	126	0.02878	0.1201	0.3305	0.4508	0.6017
7	8	168	0.02873	0.1200	0.3304	0.4506	0.6006
7	10	210	0.02872	0.1200	0.3304	0.4505	0.6005

TR = Total numbers of polynomial terms used in the r (or ψ) direction.
TZ = Total numbers of polynomial terms used in the z (or ζ) direction.
DET = Frequency determinant order.

$h/a=0.4$, and $H_b/a=4$, depicted as the last configuration in Fig. 4. One sees that the fundamental frequency (0.2471) requires using at least (TR, TZ) = (5, 12) and DET = 180 to obtain exactitude to four significant figures.

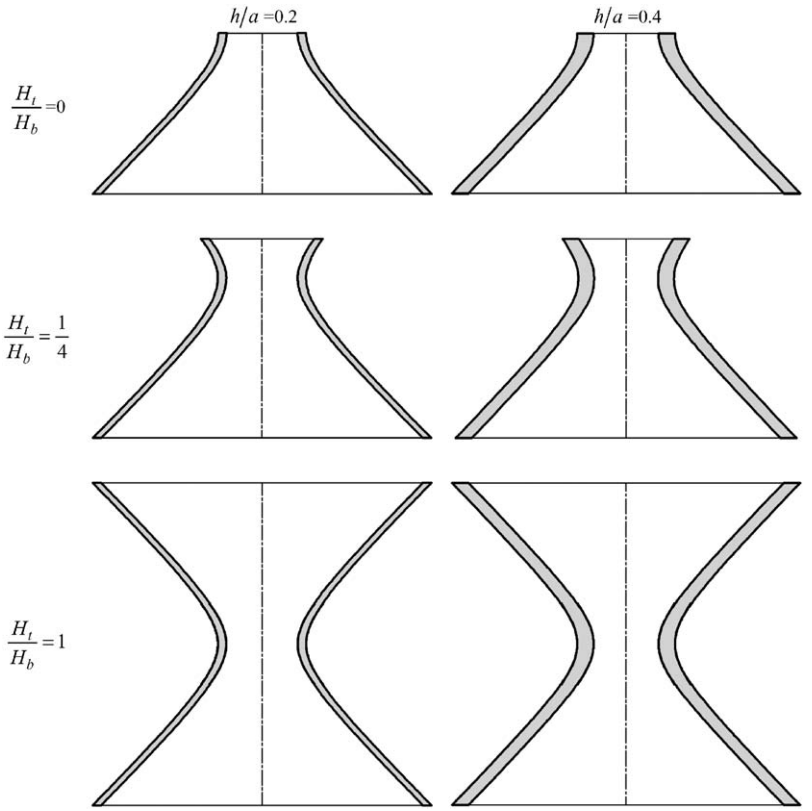

Fig. 2. Hyperboloidal shells of revolution for $b/a = 1$ and $H_b/a = 4$.

Convergence studies made for the torsional ($n = 0^T$) and axisymmetric ($n = 0^A$) modes, which are not included here, show a similar trend, with DET = 60 and 120, respectively, from (TR, TZ) = (5, 12) being needed for the first frequency to be converged up to four significant figures.

To calculate all the numerical results presented in this paper, (TR, TZ) = (5, 13) is used.

4. Numerical results and discussion

Tables 3–5 present nondimensional frequencies in $\omega a\sqrt{\rho/G}$ of completely free, hyperboloidal shells of revolution for $b/a = 1$ (Table 3), 2 (Table 4), and 3 (Table 5), and $H_b/a = 4$, having three types of top and bottom height ratios of $H_t/H_b = 0$, 1/4, and 1, and two different thickness ratios of $h/a = 0.2$ and 0.4. Poisson's ratio (ν) was taken to be 0.3. These configurations corresponding to Tables 3–5 are depicted in Figs. 2–4, respectively. Thirty-five frequencies are given for each configuration, which arise from seven circumferential wave numbers ($n = 0^T$, 0^A, 1, 2, 3, 4, 5) and the first five modes ($s = 1, 2, 3, 4, 5$) for each value of n, where the superscripts T and A indicate torsional and axisymmetric modes, respectively. The first five

Table 2
Convergence of frequencies in $\omega a\sqrt{\rho/G}$ of a completely free hyperboloidal shell of revolution for the five lowest bending modes ($n=2$) with $b/a=3$, $h/a=0.4$, $H_b/a=4$, and $H_t/H_b=1$ ($\nu=0.3$)

TR	TZ	DET	1	2	3	4	5
2	2	12	0.4727	0.6217	1.543	1.631	2.492
2	4	24	0.2824	0.2999	0.6341	0.8836	1.465
2	6	36	0.2655	0.2741	0.4991	0.6029	0.9941
2	8	48	0.2632	0.2674	0.4879	0.5581	0.8340
2	10	60	0.2624	0.2668	0.4867	0.5561	0.8012
2	12	72	0.2621	0.2664	0.4865	0.5556	0.7997
3	2	18	0.4448	0.5868	1.540	1.629	2.483
3	4	36	0.2660	0.2795	0.5700	0.7724	1.455
3	6	54	0.2513	0.2605	0.4648	0.5631	0.9102
3	8	72	0.2493	0.2546	0.4505	0.5221	0.7833
3	10	90	0.2487	0.2537	0.4494	0.5184	0.7585
3	12	108	0.2486	0.2536	0.4493	0.5181	0.7543
4	2	24	0.4438	0.5809	1.540	1.628	2.481
4	4	48	0.2648	0.2782	0.5633	0.7580	1.451
4	6	72	0.2490	0.2565	0.4617	0.5530	0.8951
4	8	96	0.2477	0.2532	0.4459	0.5198	0.7779
4	10	120	0.2473	0.2524	0.4448	0.5149	0.7555
4	12	144	0.2472	0.2522	0.4445	0.5141	0.7495
5	2	30	0.4436	0.5804	1.540	1.628	2.481
5	4	60	0.2647	0.2780	0.5618	0.7532	1.451
5	6	90	0.2487	0.2562	0.4588	0.5503	0.8867
5	8	120	0.2474	0.2528	0.4452	0.5173	0.7669
5	10	150	0.2472	0.2523	0.4444	0.5144	0.7521
5	12	180	**0.2471**	**0.2521**	**0.4443**	**0.5139**	0.7487
5	13	195	0.2471	0.2521	0.4443	0.5139	0.7480
5	14	210	0.2471	0.2521	0.4443	0.5139	**0.7479**
6	2	36	0.4436	0.5803	1.540	1.628	2.481
6	4	72	0.2646	0.2777	0.5610	0.7525	1.451
6	6	108	0.2486	0.2560	0.4580	0.5486	0.8853
6	8	144	0.2474	0.2528	0.4451	0.5171	0.7661
6	10	180	0.2472	0.2522	0.4444	0.5142	0.7509
6	12	216	0.2471	0.2521	0.4443	0.5139	0.7484
7	2	42	0.4436	0.5801	1.540	1.628	2.481
7	4	84	0.2645	0.2776	0.5596	0.7513	1.451
7	6	126	0.2486	0.2558	0.4576	0.5484	0.8850
7	8	168	0.2474	0.2527	0.4451	0.5170	0.7643
7	10	210	0.2472	0.2522	0.4444	0.5142	0.7506

TR = Total numbers of polynomial terms used in the r (or ψ) direction.
TZ = Total numbers of polynomial terms used in the z (or ζ) direction.
DET = Frequency determinant order.

frequencies for each configuration are in bold face type, and the numbers in parentheses identify the sequence of the frequencies. The zero frequencies of rigid body modes are omitted from the table.

Table 3
Frequencies in $\omega a\sqrt{\rho/G}$ of completely free, hyperboloidal shells of revolution with $b/a = 1$ and $H_b/a = 4$ for $\nu = 0.3$

		$H_t/H_b = 0$		$H_t/H_b = 1/4$		$H_t/H_b = 1$	
n	s	$h/a = 0.2$	$h/a = 0.4$	$h/a = 0.2$	$h/a = 0.4$	$h/a = 0.2$	$h/a = 0.4$
0^T	1	0.7841	0.7835	0.5547	0.5561	0.1054	0.1067
	2	1.298	1.299	0.9701	0.9730	0.7841	0.7836
	3	1.872	1.875	1.507	1.511	0.9392	0.9408
	4	2.469	2.473	2.024	2.028	1.298	1.299
	5	3.074	3.077	2.527	2.532	1.555	1.558
0^A	1	0.3140	0.3255	0.3098	0.3193	0.2400	0.2416
	2	0.4207	0.4792	0.4087	0.4598	0.3140	0.3255
	3	0.5615	0.6950	0.5438	0.6708	0.3474	0.3779
	4	0.7183	0.8687	0.7008	0.8124	0.4207	0.4792
	5	0.8623	1.027	0.8076	0.9310	0.4814	0.5763
1	1	0.3285	0.3520	0.3126	0.3265	0.09520	**0.09967(3)**
	2	0.4450	0.5240	0.3966	0.4494	0.2779	0.2845
	3	0.5782	0.6053	0.5080	0.5448	0.3374	0.3706
	4	0.6111	0.7449	0.5515	0.6489	0.3629	0.3952
	5	0.7456	0.8966	0.6625	0.7332	0.4594	0.5256
2	1	**0.02871(1)**	**0.04991(1)**	**0.03376(1)**	**0.05482(1)**	**0.03301(1)**	**0.05560(1)**
	2	**0.1200(4)**	**0.2016(4)**	**0.1383(5)**	**0.2168(4)**	**0.03695(2)**	**0.05589(2)**
	3	0.3303	0.4294	0.3296	0.4432	0.1490	0.2184
	4	0.4505	0.6143	0.4130	0.5107	0.1986	0.2469
	5	0.6003	0.7106	0.4493	0.6512	0.3510	0.4623
3	1	**0.05879(2)**	**0.1021(2)**	**0.05922(2)**	**0.1023(2)**	**0.05887(3)**	**0.1021(4)**
	2	0.1924	0.3176	0.1971	0.3202	**0.05973(4)**	**0.1024(5)**
	3	0.3757	0.5937	0.3825	0.6014	0.1952	0.3190
	4	0.5333	0.8583	0.5300	0.8636	0.2000	0.3219
	5	0.7070	0.9123	0.6052	0.9014	0.3786	0.5973
4	1	**0.09140(3)**	**0.1687(3)**	**0.09141(3)**	**0.1687(3)**	**0.09141(5)**	0.1687
	2	0.2482	0.4379	0.2484	0.4380	0.09141	0.1687
	3	0.4443	0.7584	0.4454	0.7595	0.2484	0.4380
	4	0.6416	1.087	0.6455	1.090	0.2485	0.4381
	5	0.8654	1.130	0.8595	1.132	0.4452	0.7592
5	1	**0.1339(5)**	**0.2524(5)**	**0.1339(4)**	**0.2524(5)**	0.1339	0.2524
	2	0.3172	0.5768	0.3172	0.5769	0.1339	0.2524
	3	0.5315	0.9359	0.5317	0.9361	0.3172	0.5768
	4	0.7580	1.308	0.7586	1.309	0.3172	0.5769
	5	1.013	1.356	1.019	1.357	0.5316	0.9360

T = torsional mode; A = axisymmetric mode.
Numbers in parentheses identify frequency sequence.

From Tables 3–5, for each configuration of Figs. 2–4, the following observations are noted:

1. The bending modes for $n = 2$ are seen to be the most significant, having two or three such modes among the first five frequencies, including the fundamental one, while the axisymmetric mode frequencies ($n = 0^A$) are all higher.

Table 4
Frequencies in $\omega a\sqrt{\rho/G}$ of completely free, hyperboloidal shells of revolution with $b/a = 2$ and $H_b/a = 4$ for $\nu = 0.3$

		$H_t/H_b = 0$		$H_t/H_b = 1/4$		$H_t/H_b = 1$	
n	s	$h/a = 0.2$	$h/a = 0.4$	$h/a = 0.2$	$h/a = 0.4$	$h/a = 0.2$	$h/a = 0.4$
0^T	1	0.7922	0.7915	0.5775	0.5776	**0.2061(5)**	**0.2077(3)**
	2	1.500	1.501	1.182	1.184	0.7922	0.7915
	3	2.241	2.243	1.795	1.796	1.124	1.125
	4	2.985	2.987	2.399	2.401	1.500	1.501
	5	3.730	3.731	3.002	3.004	1.869	1.872
0^A	1	0.6939	0.7060	0.6794	0.6876	0.4766	0.4776
	2	0.8641	0.9372	0.8289	0.8838	0.6939	0.7060
	3	1.094	1.252	1.025	1.106	0.7315	0.7570
	4	1.311	1.324	1.170	1.275	0.8641	0.9375
	5	1.330	1.528	1.315	1.503	0.9245	1.009
1	1	0.6570	0.6821	0.5154	**0.5267(4)**	0.2080	**0.2126(4)**
	2	0.7778	0.7930	0.7317	0.7410	0.4547	0.4640
	3	0.8816	1.007	0.7685	0.8391	0.6956	0.7332
	4	1.112	1.169	0.9765	1.130	0.7192	0.7402
	5	1.189	1.377	1.145	1.178	0.8077	0.8371
2	1	**0.08463(1)**	**0.1531(1)**	**0.09176(1)**	**0.1584(1)**	**0.09133(1)**	**0.1576(1)**
	2	**0.2037(3)**	**0.3707(3)**	**0.2177(3)**	**0.3857(3)**	**0.1004(2)**	**0.1625(2)**
	3	0.4774	**0.6491(5)**	0**.3485(5)**	**0.5287(5)**	0.2265	0.3844
	4	0.7565	1.007	0.5830	0.7906	0.2738	0.4162
	5	1.053	1.145	0.8378	1.142	0.4942	0.6773
3	1	**0.1947(2)**	**0.3531(2)**	**0.1950(2)**	**0.3532(2)**	**0.1949(3)**	**0.3532(5)**
	2	**0.4269(5)**	0.7404	0.4309	0.7427	**0.1952(4)**	0.3533
	3	0.6752	1.129	0.6852	1.145	0.4281	0.7416
	4	0.8507	1.365	0.7157	1.195	0.4351	0.7445
	5	1.135	1.545	0.9278	1.474	0.6937	1.143
4	1	**0.3320(4)**	**0.6065(4)**	**0.3320(4)**	0.6065	0.3320	0.6066
	2	0.6482	1.120	0.6484	1.121	0.3320	0.6066
	3	0.9778	1.618	0.9806	1.621	0.6484	1.121
	4	1.233	1.942	1.205	1.944	0.6486	1.121
	5	1.430	2.027	1.265	1.975	0.9797	1.623
5	1	0.5043	0.9047	0.5043	0.9048	0.5044	0.9048
	2	0.9012	1.528	0.9013	1.528	0.5044	0.9049
	3	1.287	2.090	1.287	2.090	0.9013	1.528
	4	1.639	2.371	1.642	2.371	0.9014	1.528
	5	1.927	2.606	1.817	2.610	1.287	2.091

T = torsional mode; A = axisymmetric mode.
Numbers in parentheses identify frequency sequence.

2. As the shell thickness ratio (h/a) becomes larger, all the frequencies are increased except for the first torsional modes ($n = 0^T$) for $H_t/H_b = 0$ and the second torsional ones for $H_t/H_b = 1$.

Table 5
Frequencies in $\omega a\sqrt{\rho/G}$ of completely free, hyperboloidal shells of revolution with $b/a = 3$ and $H_b/a = 4$ for $\nu = 0.3$

		$H_t/H_b = 0$		$H_t/H_b = 1/4$		$H_t/H_b = 1$	
n	s	$h/a = 0.2$	$h/a = 0.4$	$h/a = 0.2$	$h/a = 0.4$	$h/a = 0.2$	$h/a = 0.4$
0^T	1	0.7689	**0.7686(5)**	0.5801	**0.5803(5)**	**0.2697(5)**	**0.2712(4)**
	2	1.540	1.540	1.222	1.222	0.7689	0.7686
	3	2.314	2.315	1.848	1.849	1.151	1.152
	4	3.088	3.088	2.471	2.472	1.540	1.540
	5	3.861	3.861	3.093	3.094	1.927	1.928
0^A	1	0.9515	0.9596	0.8895	0.8913	0.5525	0.5528
	2	1.096	1.142	1.023	1.049	0.9515	0.9596
	3	1.294	1.383	1.205	1.276	0.9858	1.003
	4	1.454	1.516	1.387	1.496	1.096	1.142
	5	1.523	1.606	1.522	1.577	1.167	1.238
1	1	0.7620	0.7842	**0.5649(5)**	**0.5763(4)**	**0.2514(4)**	**0.2559(3)**
	2	0.8613	0.8728	0.8054	0.8199	0.5206	0.5313
	3	1.072	1.191	0.9711	1.026	0.7996	0.8290
	4	1.305	1.392	1.146	1.262	0.8538	0.8637
	5	1.418	1.579	1.297	1.393	0.9678	0.9839
2	1	**0.1320(1)**	**0.2443(1)**	**0.1373(1)**	**0.2482(1)**	**0.1358(1)**	**0.2471(1)**
	2	**0.2362(2)**	**0.4395(2)**	**0.2427(2)**	**0.4502(2)**	**0.1482(2)**	**0.2521(2)**
	3	**0.4981(4)**	**0.6899(4)**	**0.3647(4)**	**0.5604(3)**	**0.2395(3)**	**0.4443(5)**
	4	0.8641	1.132	0.6599	0.8884	0.3361	0.5139
	5	1.227	1.435	0.9731	1.296	0.5447	0.7479
3	1	**0.3246(3)**	**0.5907(3)**	**0.3248(3)**	0.5908	0.3248	0.5908
	2	0.5654	0.9854	0.5690	0.9881	0.3249	0.5908
	3	0.7318	1.249	0.7003	1.220	0.5684	0.9879
	4	0.9606	1.508	0.8198	1.347	0.5711	0.9889
	5	1.315	1.925	1.066	1.654	0.7434	1.266
4	1	**0.5734(5)**	1.018	0.5734	1.018	0.5735	1.018
	2	0.9222	1.552	0.9225	1.552	0.5735	1.019
	3	1.203	1.971	1.211	1.979	0.9224	1.552
	4	1.359	2.187	1.271	2.086	0.9227	1.552
	5	1.632	2.458	1.454	2.295	1.208	1.976
5	1	0.8787	1.504	0.8788	1.504	0.8789	1.504
	2	1.327	2.147	1.327	2.147	0.8790	1.504
	3	1.690	2.647	1.691	2.648	1.327	2.147
	4	1.945	2.981	1.924	2.982	1.327	2.147
	5	2.127	3.102	1.991	3.011	1.692	2.649

T = torsional mode; A = axisymmetric mode.
Numbers in parentheses identify frequency sequence.

3. As the curvature becomes larger (i.e., as b/a becomes smaller), most of the frequencies are decreased (for a fixed inner radius a).
4. As the curvature becomes smaller and shell thickness becomes thicker, the torsional modes ($n = 0^T$) and bending modes for $n = 1$ become more significant.

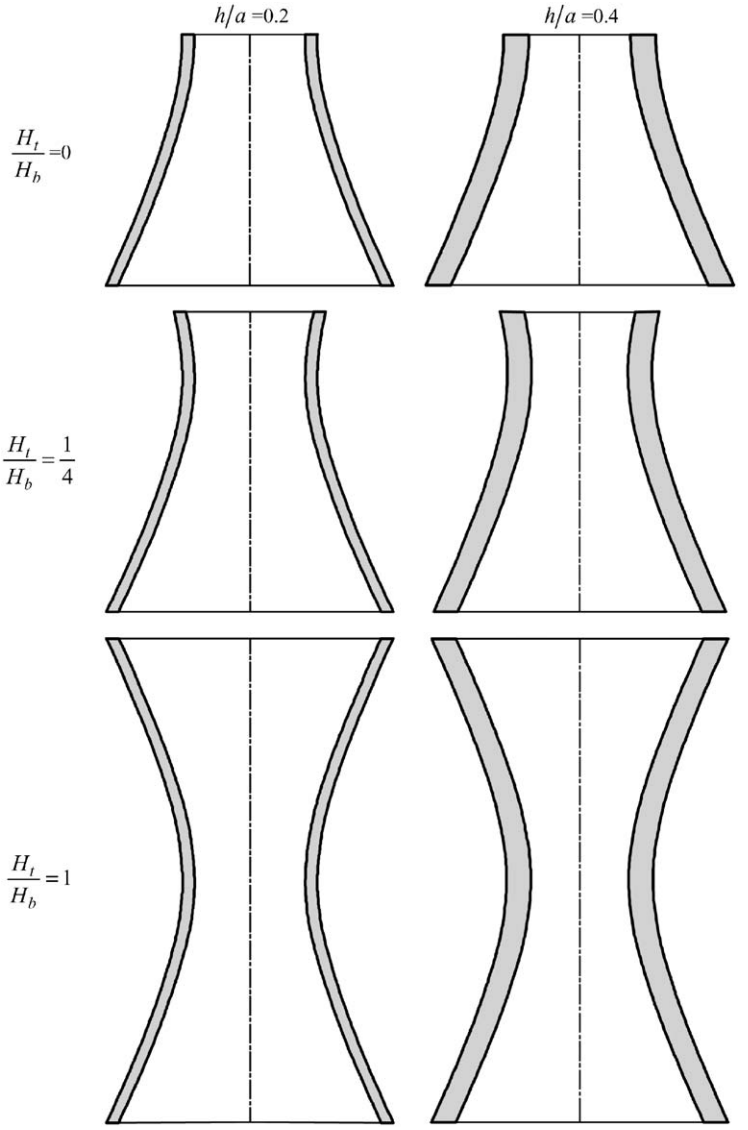

Fig. 3. Hyperboloidal shells of revolution for $b/a = 2$ and $H_b/a = 4$.

5. When hyperboloidal shells of revolution without a top portion ($H_t/H_b = 0$) are compared with ones with a small top portion ($H_t/H_b = 1/4$), the frequencies for higher circumferential wave number ($n \geqslant 2$) are not much different, while the frequencies for $n \geqslant 1$ have a large difference.
6. For each configuration with $H_t/H_b = 1$ and for $n \geqslant 3$, the first and second frequencies are nearly the same, as are the third and fourth ones. These similarities are seen to a lesser extent for $n = 2$, but become stronger as n increases.

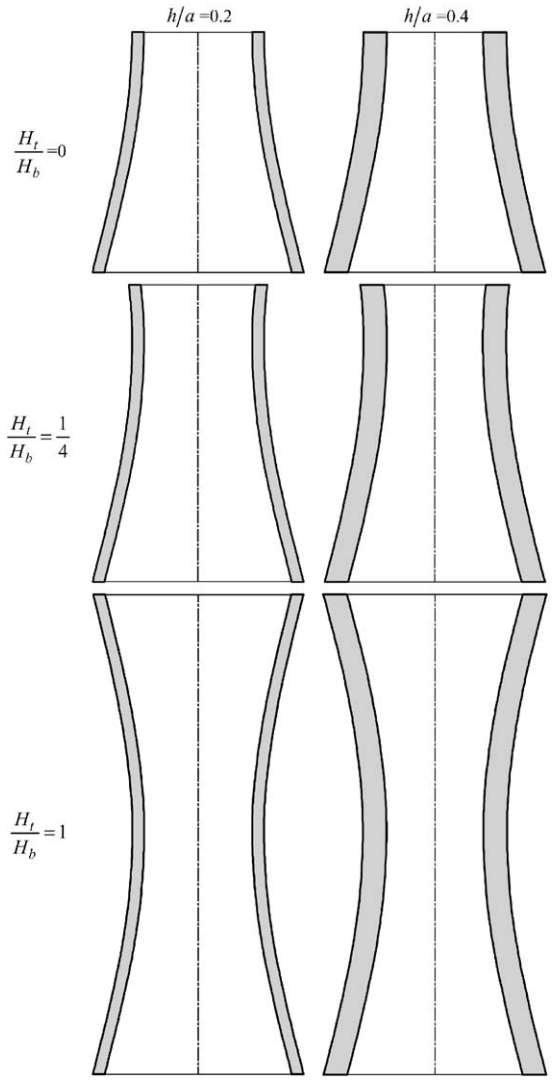

Fig. 4. Hyperboloidal shells of revolution for $b/a = 3$ and $H_b/a = 4$.

7. As the curvature becomes greater (decreasing b/a) and thickness decreases, frequencies for higher Fourier components ($n > 2$) become more significant.

5. Cylindrical and nearly cylindrical shells

It would be interesting to compare the frequencies of the longitudinally symmetric ($H_t/H_b = 1$) hyperboloidal shells with those of circular cylindrical shells having the same middle radius (a), length (H) and thickness (h). The latter shells are obtained in the present analysis by letting $b/a \rightarrow$

Table 6
Frequencies in $\omega a\sqrt{\rho/G}$ for nearly cylindrical ($b/a = 10$) and cylindrical ($b/a = 1000$) shells with $H/a = 8$ for $\nu = 0.3$

		$b/a = 10$		$b/a = 1000$	
n	s	$h/a = 0.2$	$h/a = 0.4$	$h/a = 0.2$	$h/a = 0.4$
0^T	1	**0.3749(5)**	**0.3752(2)**	**0.3927(5)**	**0.3927(2)**
	2	0.7774	0.7776	0.7854	0.7854
	3	1.173	1.173	1.178	1.178
	4	1.567	1.567	1.571	1.571
	5	1.960	1.960	1.964	1.964
0^A	1	0.6195	0.6194	0.6281	0.6280
	2	1.194	1.194	1.201	1.201
	3	1.470	1.478	1.506	1.515
	4	1.505	1.514	1.579	1.597
	5	1.519	1.535	1.603	1.618
1	1	**0.2968(4)**	**0.3013(1)**	**0.3030(3)**	**0.3075(1)**
	2	0.5861	0.5984	0.5940	0.6065
	3	0.8649	0.8934	0.8729	0.9018
	4	0.9802	1.000	0.9970	1.018
	5	1.160	1.191	1.184	1.220
2	1	**0.2392(1)**	**0.4523(3)**	**0.2557(1)**	**0.4849(3)**
	2	**0.2411(2)**	**0.4533(4)**	**0.2615(2)**	**0.4937(4)**
	3	**0.2931(3)**	**0.5233(5)**	**0.3095(4)**	**0.5466(5)**
	4	0.4240	0.6509	0.4395	0.6761
	5	0.6168	0.8592	0.6294	0.8808
3	1	0.6444	1.146	0.7011	1.245
	2	0.6445	1.146	0.7081	1.254
	3	0.7171	1.264	0.7405	1.298
	4	0.7693	1.325	0.8041	1.378
	5	0.8710	1.448	0.9058	1.501
4	1	1.177	1.966	1.292	2.144
	2	1.178	1.967	1.298	2.150
	3	1.297	2.146	1.330	2.192
	4	1.329	2.179	1.384	2.258
	5	1.407	2.275	1.464	2.355
5	1	1.812	2.851	1.994	3.110
	2	1.813	2.852	2.000	3.114
	3	1.985	3.089	2.031	3.155
	4	2.003	3.104	2.082	3.211
	5	2.076	3.193	2.153	3.293

T = torsional mode; A = axisymmetric mode.
Numbers in parentheses identify frequency sequence.

∞. It is noted that cylindrical shells are of zero Gaussian curvature while hyperboloidal shells have negative Gaussian curvature.

Table 6 presents $\omega a\sqrt{\rho/G}$ for hyperboloidal shells having $b/a = 1000$. These are essentially cylindrical. Let the R be the shell radius (r) at $z = \pm H/2$ (Fig. 1); i.e., at the ends of the shell. How

nearly a hyperboloidal shell is cylindrical is clearly seen by examining the ratio of this radius to the middle radius; i.e., R/a. From the equation for the hyperbolic mid-surface one obtains

$$\left(\frac{R}{a}\right)^2 = 1 + \left(\frac{H}{2b}\right)^2 = 1 + \left(\frac{H}{2a}\right)^2\left(\frac{a}{b}\right)^2. \tag{20}$$

For $H/a = 8$, which corresponds to the $H_b/a = 4$ used in Tables 3–5, Eq. (20) becomes

$$\left(\frac{R}{a}\right)^2 = 1 + 16\left(\frac{a}{b}\right)^2. \tag{21}$$

Thus, using $b/a = 1000$ for Table 6 in Eq. (21) gives $R/a = 1.000008$. Since the outer radius (R) and middle one (a) are then essentially the same, the shell is essentially cylindrical.

At the same time, it is easy to demonstrate to what extent the presence of a small meridional curvature may change the frequencies of a cylindrical shell, which has circumferential curvature (radius of curvature a). For this purpose, results are also shown in Table 6 for $b/a = 10$. From Eq. (21), this corresponds to a shell radius R at the outer ends of this slightly hyperboloidal (nearly cylindrical) shell, which is 1.077 times the middle radius (a).

In Table 6, one sees that the presence of a small meridional curvature ($b/a = 10$) causes the following changes in the frequencies, compared to those of a cylindrical shell ($b/a = 1000$):

1. All frequencies are decreased.
2. The axisymmetric ($n = 0^A$) and first flexural ($n = 1$) mode frequencies change very little ($<2\%$).
3. Torsional frequencies change more ($<4\%$).
4. Significant changes occur for the higher flexural modes ($n > 1$); for example, a frequency decrease of 9.1% is seen for $n = 5$ when $h/a = 0.2$.

The trends described above are extendable further to increasing the meridional curvature by comparing directly with the data for $b/a = 3$ (Table 5, with $H_t/H_b = 1$).

It is interesting to note that the nearly degenerate (equal frequency) modes observed in Tables 3–5 for $n > 2$ and $H_t/H_b = 1$ become more separated in Table 6 as the shell becomes more nearly cylindrical.

To establish further the accuracy of representing a cylindrical shell by $b/a = 1000$, Table 7 is added, which compares $\omega a\sqrt{\rho/G}$ obtained by the present method with accurate values obtained by a 3-D analysis carried out in cylindrical coordinates [27]. The accuracy of the latter method was partly established in Ref. [27] by comparison with results obtained by others, using other analytical methods, and experimentally. In Table 7, frequencies are presented for $h/a = 2/19$ (≈ 0.1053), and for two H/a ratios, $40/19 (\approx 2.105)$ and $200/19 (\approx 10.53)$. One sees close agreement between the results for $b/a = 1000$ and the hollow cylinders.

6. Conclusions

Accurate frequency data determined by the 3-D Ritz analysis have been presented for thick hyperboloidal shells of revolution. The analysis uses the 3-D dynamic equations of the theory of elasticity in their general forms for isotropic materials. They are only limited to small strains. No

Table 7
Comparison of present method ($b/a = 1000$) and 3-D hollow cylinder [27] frequencies $\omega a\sqrt{\rho/G}$, for $h/a = 2/19$ (≈ 0.1053), $\nu = 0.3$

		$H/a = 40/19$ (≈ 2.105)		$H/a = 200/19$ (≈ 10.53)	
n	s	$b/a = 1000$	Cylinder [27]	$b/a = 1000$	Cylinder [27]
0^T	1	1.492	1.492	0.2984	0.2985
	2	2.985	2.985	0.5969	0.5969
	3	4.477	4.477	0.8954	0.8954
	4	5.969	5.969	1.194	1.194
	5	7.462	7.461	1.492	1.492
0^A	1	1.564	1.564	0.4791	0.4792
	2	1.606	1.606	0.9408	0.9409
	3	1.622	1.622	1.325	1.325
	4	1.732	1.732	1.509	1.509
	5	2.060	2.060	1.565	1.564
1	1	1.229	1.229	0.1917	0.1917
	2	1.410	1.410	0.4127	0.4127
	3	1.681	1.681	0.6403	0.6403
	4	2.049	2.049	0.8318	0.8318
	5	2.057	2.057	0.9946	0.9946
2	1	0.1356	0.1356	0.1367	0.1367
	2	0.1759	0.1759	0.1385	0.1385
	3	1.035	1.035	0.1623	0.1623
	4	1.507	1.507	0.2401	0.2400
	5	1.872	1.872	0.3634	0.3633
3	1	0.3799	0.3799	0.3830	0.3830
	2	0.4430	0.4429	0.3853	0.3852
	3	0.9163	0.9162	0.3971	0.3970
	4	1.504	1.503	0.4229	0.4227
	5	2.140	2.138	0.4691	0.4688
4	1	0.7195	0.7195	0.7251	0.7250
	2	0.7909	0.7909	0.7272	0.7270
	3	1.114	1.113	0.7389	0.7388
	4	1.661	1.659	0.7591	0.7589
	5	2.324	2.322	0.7899	0.7896
5	1	1.146	1.146	1.154	1.154
	2	1.220	1.219	1.156	1.156
	3	1.500	1.498	1.169	1.168
	4	1.988	1.986	1.188	1.187
	5	2.635	2.633	1.216	1.215

T = torsional mode; A = axisymmetric mode.

other constraints are placed upon the displacements. This is in stark contrast with the classical 2-D shell theories, which make very limiting assumptions about the displacement variation through the thickness.

Convergence of the method was demonstrated by obtaining frequencies to four significant figures of exactitude for a typical Fourier component ($n=2$), which includes the fundamental frequency, of two representative hyperboloidal shells of revolution that are completely free. The method was then used to compute accurate and extensive frequencies for three sets of completely free, hyperboloidal shells of revolution, which are of large ($b/a=1$), moderate ($b/a=2$), and small ($b/a=3$) curvatures. This type of problem has no known solution in the published literature.

The energy formulation using the Ritz method is a particularly good approach for structural problems to find static displacements, free vibration frequencies and mode shapes, and buckling loads and mode shapes. Accurate stress determination by the method is questionable in 3-D analyses, however, especially for shapes having large stress gradients (sharp internal corners, cracks, etc.) because the stresses involve derivatives of the displacements.

Although correctly developed and properly used finite element methods can obtain reasonably accurate frequencies, even in 3-D representations, they typically require many more degrees of freedom (i.e., much larger sizes of eigenvalue determinants to evaluate) to achieve comparable accuracy. This was demonstrated extensively in a paper by McGee and Leissa [26]. The Ritz method guarantees upper bound convergence of the frequencies in terms of functions sets that are mathematically complete, such as algebraic polynomials. Some finite element methods can also accomplish this, but at much greater costs, and others cannot.

References

[1] A.W. Leissa, *Vibration of Shells*, US Government Printing Office, Washington, DC, 1973 (reprinted by The Acoustical Society of America, 1993).
[2] Anon, Report of the Committee of Inquiry into Collapse of Cooling Towers at Ferrybridge Monday 1 November, Central Electricity Generating Board, London, England, 1965.
[3] B.G. Neal, Natural frequencies of cooling towers, *Journal of Strain Analysis* 2 (2) (1967) 127–133.
[4] R.L. Carter, A.R. Robinson, W.C. Schnobrich, Free and forced vibrations of hyperboloidal shells of revolution, Civil Engineering Studies, Structural Research, Vol. 334, University of Illinois, 1968.
[5] S.N. Krivoshapko, Static, vibration, and buckling analyses and applications to one-sheet hyperboloidal shells of revolution, *Applied Mechanics Reviews* 55 (3) (2002) 241–270.
[6] V.I. Andronov, A.A. Boltuhov, B.N. Povolotskiy, Natural vibrations of cooling tower shells, *Stroit. meh. i raschet soor.* 4 (1966) 16–19 (in Russian).
[7] J.E. Stoneking, Free vibrations of shells of revolution with variable thickness, *Nuclear Engineering and Design* 24 (1973) 314–321.
[8] K. Sen Subir, L. Gould Phillip, Free vibration of shells of revolution using FEM, *Journal of the Engineering Mechanics Division* 100 (2) (1974) 283–303.
[9] A.I. Tupikin, A free vibration investigation of a cooling tower shell with the help of a finite element method, *Trudy, TsNIISKa* 43 (1975) 28–46 (in Russian).
[10] P.L. Gould, P.K. Basu, Dynamische Untersuchung von Naturzugkühltürmen, *Konstruktiver Ingenieurbau Berichte* 31 (1978) 82–83.
[11] R.L. Nelson, D.L. Thomas, Free vibration analysis of cooling towers with column supports, *Journal of Sound and Vibration* 57 (1) (1978) 149–153.
[12] L.I. Lyahina, Natural frequencies and modes of a hyperboloidal cooling tower shell with local axisymmetrical imperfections, *MKE raschotah zhelezob. plastin i obol.*, Frunze, FPI, 1979, pp. 118–126 (in Russian).
[13] R. Delpak, W.M. Hague, An experimental and theoretical investigation of the frequencies and mode shapes of axisymmetric shell models, *Journal of Sound and Vibration* 72 (1980) 235–249.

[14] R. Nelson, Stresses in shell structures, *Journal of Sound and Vibration* 79 (3) (1981) 397–414.
[15] G.I. Belikov, A.A. Tarasov, Free vibration optimization of geometric parameters of cooling tower shells, *Stroit. mech. i raschet sooruzheniy* 4 (1982) 12–16 (in Russian).
[16] V.D. Kustovskiy, A finite element solution of free vibration problems for thin elastic shells of revolution bounded by parallels, *Nadezhnost sudov. mashin, Nikolaev*: NKI, 1983, pp. 54–65 (in Russian).
[17] N.V. Kolkunov, E.M. Zveryaev, Cooling tower shell dynamics, *International Congress Teoriya i eksper. issled. prostranst. konstruktsiy, Primenenie obolochek v ing. soor*, Vol. 3, Moscow, 1985, pp. 146–155 (in Russian).
[18] T. Kosawada, K. Suzuki, S. Takahashi, Axisymmetric free vibrations of shells of revolution having general meridional curvature, *Transactions of the JSME* C52 (473) (1986) 209–215 (in Japanes).
[19] A.N. Lin, H. Mozaffarian, M. Helpingstine, Measured dynamic response of hyperbolic shell, *Proceedings of the Third US National Conferencee on Earthquake Engineerings*, Charleston, SC, Vol. 2, El Cerrito, CA, 1986, pp. 1407–1418.
[20] Loo Wenda, Gao Shi-qiao, The effect of local geometric imperfections of rational shell on its natural frequencies and modes, *Applied Mathematics and Mechanics* 8 (11) (1987) 1013–1018.
[21] W. Abramek, Drgania wlasne hiperboloidalnej chlodni kominowej, *Inz. i bud.* 46 (9) (1989) (in Polish).
[22] Zhao Yangang, Jiang Jinren, Dynamic analysis of hyperbolic cooling towers, *Earthquake Engineering Engineering Vibration* 14 (1) (1994) 61–71 (in Chinese).
[23] I.S. Sokolnikoff, *Mathematical Theory of Elasticity*, Second Ed, McGraw-Hill, New York, 1956.
[24] L.V. Kantorovich, V.I. Krylov, *Approximate Methods in Higher Analysis*, Noordhoff, Groningen, The Netherlands, 1958.
[25] W. Ritz, Über eine neue Methode zur Lösung gewisser Variationsprobleme der mathematischen Physik, *Zeitschrift für die Reine und Angewandte Mathematik* 135 (1909) 1–61.
[26] O.G. McGee, A.W. Leissa, Three-dimensional free vibrations of thick skewed cantilever plates, *Journal of Sound and Vibration* 144 (1991) 305–322 (errata 149 (1991) 539–542).
[27] J. So, A.W. Leissa, Free vibrations of thick hollow circular cylinders from three-dimensional analysis, *Journal of Vibration and Acoustics* 119 (1997) 89–95.